Axial Dispersion in Turbulent Flow Through Standard 90 Degree Elbows

ROBERT E. CASSELL, JR.

The University of Tennessee, Knoxville, Tennessee

and

JOSEPH J. PERONA

Oak Ridge National Laboratory, Oak Ridge, *Tennessee*

Axial dispersion was studied experimentally for turbulent flow through a 1¼-in. piping system containing 90 deg. elbows. The Reynolds number range was 15,400 to 96,555. The imperfect pulse tracer technique was used with the axial dispersion numbers being obtained from the difference in variances of concentration-time curves observed at two points in the system.

Elbows interconnected by short lengths of pipe with each succeeding one reversed so as to cause a change in the direction of flow, increased axial dispersion by 35 to 61% over that expected for straight pipe, while the same elbows turned so as to form a helix decreased the dispersion substantially; however, the amount of axial dispersion was still 8 to 22% greater than that observed for straight pipe.

The equivalent lengths of the elbows depend upon both their arrangement and the Reynolds number. Closely placed, helically arranged elbows required equivalent lengths of from 2.9 to 5.1 diam., while a reversed arrangement required 6.9 to 11.6 diam. Elbows separated by a developing length and randomly arranged yielded an equivalent length range of 3.6 to 10.6 diam. The geometical *l/d* ratio of the elbows used was 2.05.

Interest in the prediction of dispersion is increasing in the chemical industry today, the widest interest being in the mixing of fluids in tubular flow reactors and in the contamination of different fluids flowing back-to-back in pipelines. Although axial dispersion of liquids in straight pipe has been studied quite extensively (*1* to *9*), dispersion during flow through pipe fittings has not been reported.

The models used to describe dispersion draw on the analogy between mixing in actual flow and a diffusional process. If the disturbances in turbulent mixing are assumed to be statistical in nature, the dispersion model can be applied by methods similar to the classical ones of heat conduction and diffusion. G. I. Taylor derived a useful equation relating the physical variables of the flow system to the dispersion coefficient (*6*). Several extensions and generalizations of his equation have been performed (*10* to *12*), the most important ones summarized by Bischoff and Levenspiel (*13, 14*).

There has been only one study dealing with 90 deg. bends and straight pipe. In this study Bischoff (*15*) treated the bends as perfect mixers (that is, backmix sections) since dispersion data on elbows had not yet been taken. Another example of combined models is found in the work of Halwagi and Gomezplata (*16*) on gas mixing in fluidized beds, where a two-phase model was used.

The present work presents an experimental study of the dispersion due to 90 deg. elbows connected in various arrangements. A new combined model is formulated which treats the 90 deg. elbows as dispersion sections.

THEORY

The axial dispersed plug flow model is represented by the following:

$$\frac{\partial c}{\partial t} + u\frac{\partial c}{\partial x} = D_e\frac{\partial^2 c}{\partial x^2} \tag{1}$$

As developed by Levenspiel and Smith (*12*), the dispersion coefficient with a perfect impulse tracer injection is related to the variance of the output concentration-time curve by

$$\sigma^2 = \frac{2D_e}{uL} \tag{2}$$

Aris (*10*) showed that the shape of the input pulse was arbitrary if the difference in variances was used, and Bischoff (*17*) generalized this to apply to any model.

In the combined model, all of the straight pipe dispersion sections are represented by

$$\left(\frac{L_P}{L}\right)\Delta\mu = \Delta\mu_P = \frac{L_P}{L} \tag{3}$$

and

$$\left(\frac{L_P}{L}\right)^2 \Delta\sigma^2 = \Delta\sigma_P{}^2 = 2\frac{D_P}{uL_P}\left(\frac{L_P}{L}\right)^2 \tag{3}$$

All of the standard 90 deg. elbow sections are represented by

$$\left(\frac{L_B}{L}\right)\Delta\mu = \Delta\mu_B = \frac{L_B}{L} \tag{5}$$

and

$$\left(\frac{L_B}{L}\right)^2 \Delta\sigma^2 = \Delta\sigma_B{}^2 = 2\frac{D_B}{uL_B}\left(\frac{L_B}{L}\right)^2 \tag{6}$$

In order to obtain a more useful expression for the elbow section, the dispersion is put on a straight pipe basis by replacing the true length of the elbow, L_B, by an equivalent length of straight pipe, L_{Beq}. Equations (5) and (6) thus become

$$\Delta\mu_B = \frac{L_{Beq}}{L} \tag{7}$$

$$\Delta\sigma_B{}^2 = 2\frac{D_P}{uL_{Beq}}\left(\frac{L_{Beq}}{L}\right)^2 \tag{8}$$

The ratios of lengths in Equations (3) through (8) are used to put the moments on the same dimensionless basis.

Robert E. Cassell, Jr. is with Tennessee Eastman Company, Kingsport, Tennessee. Joseph J. Perona is at the University of Tennessee, Knoxville, Tennessee.

In order to relate the overall dispersion model (using the effective axial dispersion coefficient for the entire system) to the combined model that considers the detailed parts of the system, the knowledge that the mean and variance for a set of linearly connected independent distributions are additive is used. Thus for the total combined model, Equations (3), (4), (7), and (8) when added yield

$$\Delta\mu = \frac{L_P}{L} + \frac{L_{Beq}}{L} = 1 \tag{9}$$

$$\Delta\sigma^2 = 2\frac{D_P}{uL_P}\left(\frac{L_P}{L}\right)^2 + 2\frac{D_P}{uL_{Beq}}\left(\frac{L_{Beq}}{L}\right)^2 \tag{10}$$

By equating the dimensionless second moments in Equations (2) and (10), the relationship between the individual and overall dispersion coefficients is obtained:

$$\frac{D_e}{uL} = \frac{D_P}{uL_P}\left(\frac{L_P}{L}\right)^2 + \frac{D_P}{uL_{Beq}}\left(\frac{L_{Beq}}{L}\right)^2 \tag{11}$$

Each of the geometrical factors (L_P/L) and (L_{Beq}/L) is independent of the total number of sections in the system.

By rearranging the above equation, an expression for the equivalent length of a standard 90 deg. elbow is obtained:

$$L_{Beq} = \frac{L\left[\frac{D_e}{uL} - \frac{D_P}{uL}\left(\frac{L_P}{L}\right)\right]}{\left(\frac{D_P}{uL}\right)} \tag{12}$$

EXPERIMENTAL EQUIPMENT

The flow system consisted of a centrifugal pump with attached motor, hold tank, rotameter, and various piping, valves, and fittings. All pipe, valves, and fittings were 1¼-in. size and made of stainless steel.

Water from the building's city water supply was fed into the hold tank; a constant level was maintained by means of a run-off line near the top leading to a drain. The water was pumped from the bottom of the tank through the 1¼-in pipe

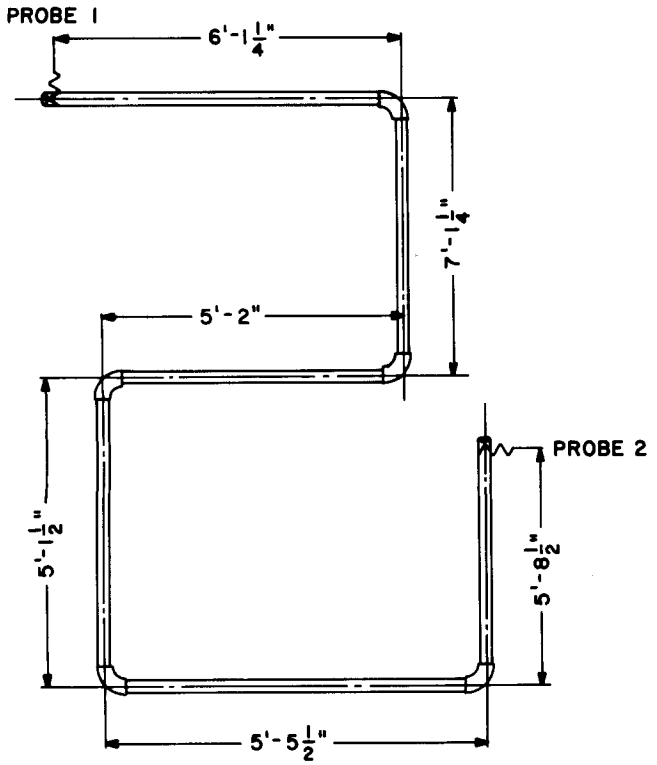

Fig. 1. The five-elbow experimental section.

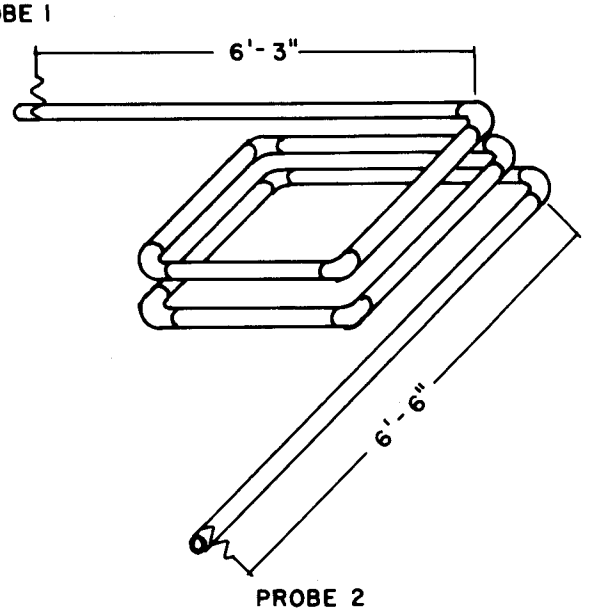

Fig. 2. The nine-elbow helical experimental section.

containing the calibrated rotameter. The flow rate was controlled by a globe valve. The inlet water temperature was measured by a thermometer immersed in the hold tank. After flowing through the straight pipe section, where the tracer was introduced, and then through the experimental section, the water and tracer mixture passed to the drain through a raised end section which was constructed to prevent the presence of air pockets in the system. The exit water temperature was measured by a thermometer immersed in the drain trough.

An experimental section was taken to be that length between the two conductivity probes. End effects were reduced by extending the beginning and end of the experimental section more than fifty pipe diameters. To be specific, the exit section was 6.5 ft. (56.52 diam.) while the entrance section was 8.167 ft. (70.84 diam.).

The first experimental section used was simply a straight pipe 12.75 ft. in length.

The second experimental section consisted of straight pipe and five 90 deg elbows arranged as shown in Figure 1. The total length of this section was 34.67 ft. A minimum developing length of 44.87 diam. was allowed between each of the five elbows.

The third experimental section was composed of straight pipe and nine 90 deg. elbows, all turned in the same direction so as to form a helical arrangement. They were separated from each other by only 5½ or 6 in. (4 diam.) pipe segments. The total length of this section was 16.5 ft. The arrangement of this experimental section is depicted in Figure 2.

The fourth, and last, experimental section is shown in Figure 3. It is merely the third section rearranged so that each of the nine elbows caused a change in direction of fluid flow. The total length of this section was also 16.5 ft.

The tracer-injection section was a 1 ft. piece of 1¼ in. stainless steel pipe fitted at each end with a stainless steel ball valve. The section was filled with 0.005N sodium nitrate tracer by gravity feed from a plexiglas tank located above the section. The sodium nitrate solution was fed through a valve on the bottom of the section until it had overflowed through holes on top. The holes were capped off and the tracer was ready for a run.

The concentration of sodium nitrate in the liquid passing through the experimental section was monitored by use of an electrical conductivity cell mounted at each end of the section. An A.C. electrical signal was applied to the electrodes in the cell, and the resistance of the flowing liquid was measured by making the cell one arm of a Wheatstone bridge. Electrical conductance was measured with a Sanborn preamplifier, amplifier, and controller.

Figure 4 is a drawing of the electrical conductivity cell used. Instead of the usual two electrodes separated by a finite distance, the cell employed substituted a 3/16 in. stainless steel rod insulated from the pipe wall as one electrode and used

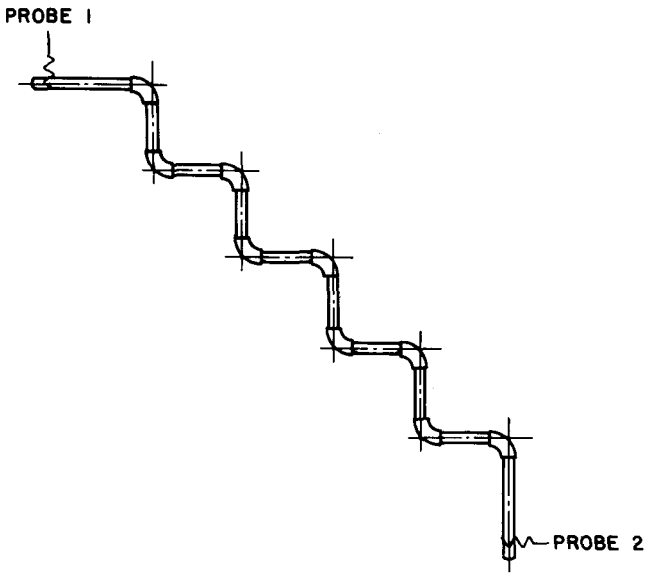

Fig. 3. The nine-elbow reversed experimental section.

the stainless steel pipe as the other electrode.

Although the exact cell constant of the conductivity cell was unimportant, the consistency of its value was important. An approximate equivalent cell constant of 0.275 was obtained in a static test cell using a 0.01N potassium chloride solution. This constant was checked periodically throughout the investigation without any observed change.

The sequence of events for a typical run was as follows. As the first step, city water was introduced into the system and the pump started. The flow rate was adjusted to that desired for the particular run. This situation was maintained until the temperature and conductivity of the water leveled out. The recording equipment was then balanced and calibrated The recording stylus was adjusted to the baseline of the chart, the desired sensitivity set, and a ball valve at the end of the flow system was closed. Immediately after that, the two ball valves on each side of the tracer injection section was simultaneously closed and the section allowed to drain of water. As soon as this section was completely emptied of water, it was refilled with 0.005N sodium nitrate solution by means of gravity feed from the overhead tank. The recording chart was started, the ball valves on each side of the tracer section was simultaneously opened, and the flow was started by opening the terminal ball valve. The concentration of the sodium nitrate tracer as a function of time was recorded as it passed the conductivity probe. Not including the time required to achieve steady state, a typical run took approximately 10 min.

The data recorded during the experimental runs were in the form of curves of the concentration of the sodium nitrate tracer as a function of time. The curves have generally the same shape, but are noticeably asymmetric at the lower Reynolds numbers, the concentration rising quickly to a maximum and then decreasing more slowly (*18*). A reason for this is that the boundary layer is rather thick at the lower Reynolds numbers and the loss of the sodium nitrate from that layer takes longer than in the case where the Reynolds number is higher. It should

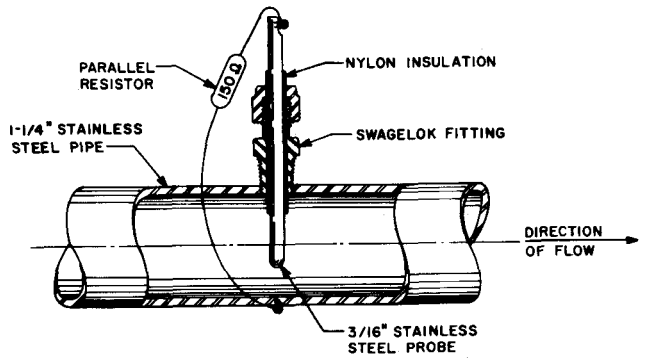

Fig. 4. The electrical conductivity cell (in line).

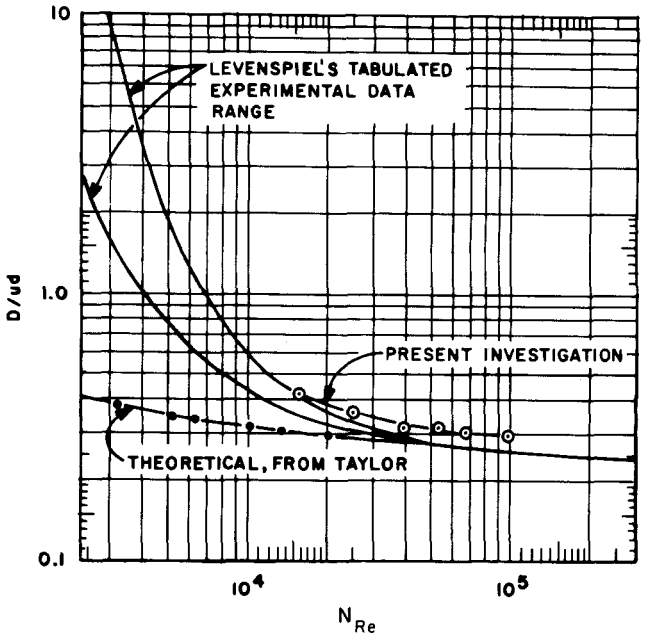

Fig. 5. Comparison of straight pipe results with those of the literature.

be pointed out that the skewness of the tracer curves was more pronounced on the readings taken at probe 1 than on those taken at probe 2. This phenomenon occurs because the dispersed pulse is increasing in length as it passes the measurement point. This factor is not important if the time taken by the tracer to reach the observation point is much greater than the time taken to pass the observation point. Obviously, this factor is decreased from the first to the second measurement point. Turner (*8*) has shown that if $l/d >> 20$ then the previous mentioned effect is unimportant.

The dimensional variances of these tracer curves were calculated by breaking the continuous curves up into a finite number of equal intervals so that the following discrete formula could be used (*19*):

$$\sigma_t^2 = \frac{\sum_{i=1}^{k} t_i^2\, C(t_i)}{\sum_{i=1}^{k} C(t_i)} - \left[\frac{\sum_{i=1}^{k} t_i\, C(t_i)}{\sum_{i=1}^{k} C(t_i)}\right]^2 \qquad (13)$$

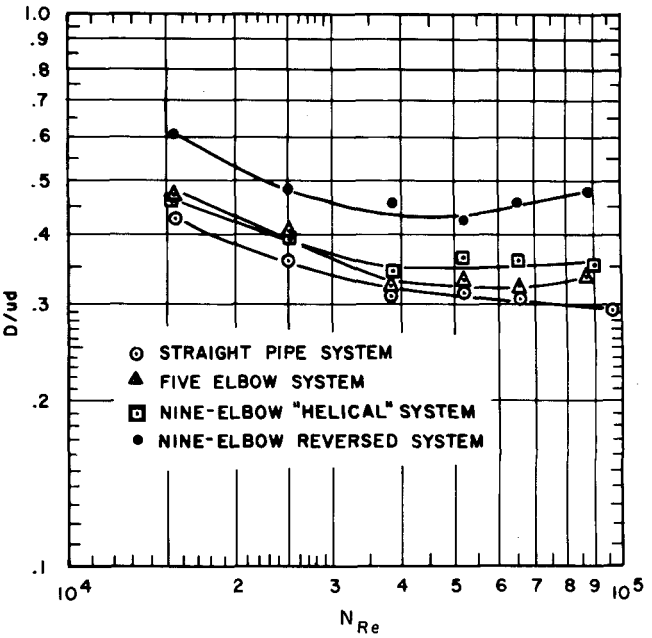

Fig. 6. Experimental and theoretical drying curves of a balsa wood with a thickness of ¼ in.

In an effort to establish the reliability of the experiments as to reproducibility with respect to previous investigations, several runs were made at different Reynolds numbers in the straight pipe system. These runs were taken over a 4-month period so that any changes in the conductivity cell constant could be observed. There was no observed change whatsoever.

RESULTS

Levenspiel's (*4*) comprehensive correlation results and Taylor's (*6*) theoretical analysis based on the diffusion model, together with the results of the present work for straight pipe are shown in Figure 5.

The dimensionless group, D/ud, is called the *axial dispersion number* and is used to place all the results, regardless of the tube length, on the same basis.

From the good agreement of the straight pipe results with the data correlated by Levenspiel (less than 15% difference), it was concluded that this system could obtain data of excellent quality for the other investigations to be performed.

The axial dispersion numbers for the two nine-elbow systems are compared with each other and the straight pipe dispersion numbers in Figure 6. As expected, all of the systems containing elbows indicated a greater degree of axial mixing than the straight pipe system. The nine-elbow reversed system seemed to be the best axial mixing system; it showed a 35 to 61% increase over that of straight pipe. The five-elbow and nine-elbow helical systems seemed to contribute only moderately to axial mixing. The former increased axial mixing by 2.5 to 12%, while the latter showed an increase of 8.4 to 22% over that of the straight pipe system. Koutsky and Adler (*20*) have shown that a true helix with constant radius of curvature and constant pitch decreases the axial mixing below that of a straight tube by 5 to 12%. There is a suggestion of minima in the curves of Figure 6 where elbows were present. This is especially true for the nine-elbow reversed case. Carter and Bir (*21*) also observed these minima for the flow of gases around return bends.

Figure 7 is a presentation of the equivalent length of a 90 deg. elbow as a function of Reynolds number. These equivalent lengths were calculated from Equation (12) using values of the axial dispersion numbers read from the smooth curves of Figure 6. In calculating the equivalent length of an elbow, it was assumed that each of the elbows present in the system contributed equally to the mixing process.

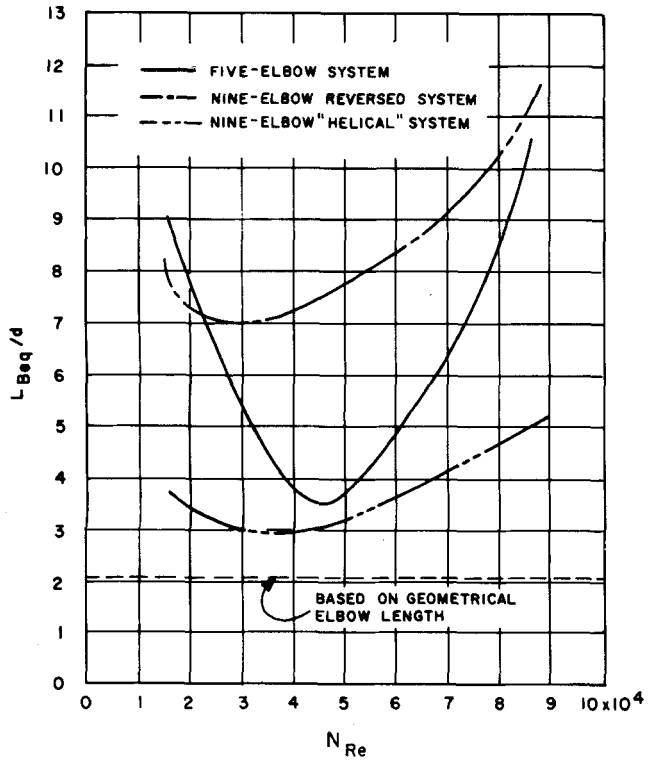

Fig. 7. Experimental and theoretical drying curves of a balsa wood with a thickness of ⅜ in.

CONCLUSIONS

The initially high equivalent length at the lower Reynolds numbers is probably due to the nonuniform velocity profile. Therefore, fluid molecules in different positions across the cross section are moving with different axial velocities. This naturally results in a high amount of axial dispersion, and, as a result, the equivalent lengths are also high. As the Reynolds number increases, turbulent eddy activity increases, and the improved radial mixing randomizes the position of molecules in the cross-sectional plane. This decreases the axial mixing and thus also the equivalent length. By means of the above two mechanisms, all three curves have been decreased. The five-elbow system shows a much more marked decrease since an adequate developing length ($l/d > 45$) was between each elbow. Therefore, the velocity profile was able to flatten out. In the two nine-elbow systems, there was not much developing length ($l/d = 4$) between the elbows, and for this reason both of the above mechanisms were reduced in their effectiveness, although they were still strong enough to show a decrease in equivalent length requirements. In a Reynolds number range of 30,000 to 50,000, each of the three curves reached a minimum and began an upswing. A possible reason for this upswing is that a separation of the flow occurs around the indicated Reynolds number range; however, no data were found in the literature to either support or discredit this idea. It is definitely believed that the mechanism of secondary flow is the cause for the entire nine-elbow helical system's equivalent length requirement being much less than that for the nine-elbow reversed system. It should be pointed out that the minimums in the five-elbow system and the helical system curve come close to the l/d ratio for the true length of the bend. This is to be expected for the reasons previously discussed.

ACKNOWLEDGMENT

The conductivity cell was constructed by the dept. of Chemical and Metallurgical Engineering shop at the Univ. of Tennessee, from a design by Tom Gayle of Oak Ridge National Laboratory.

NOTATION

C = tracer concentration, moles/cu. ft.
d = pipe diameter, ft.
D = axial dispersion coefficient, sq.ft./sec.
D_e = effective axial dispersion coefficient for entire system, sq.ft./sec.
l = a length of pipe, ft.
L = length of experimental section, ft.
L_{Beq} = length of standard 90 deg. elbow equivalent to straight pipe, ft.
N_{Re} = Reynolds number, dimensionless
t = time, sec.
u = mean flow velocity, ft./sec.
x = axial poition, ft.

Greek Letters

μ = first moment about the origin, dimensionless
σ^2 = variance = second moment about the mean, dimensionless

σ_t^2 = dimensionless variance, sq. sec.

Subscripts

B = standard 90 deg. elbow
P = straight pipe

LITERATURE CITED

1. Hawthorn, R. D., *AIChE J.*, **6**, 443 (1960).
2. Hull, D. E., and J. W. Kent, *Ind. Eng. Chem.*, **44**, 2745 (1952).
3. Levenspiel, O., *Petrol. Refiner*, **37**, 191 (1958).
4. ———, *Ind. Eng. Chem.*, **50**, 343 (Mar., 1958).
5. Sjenitzer, F., *Pipeline Eng.*, **30**, D31 (Dec., 1958).
6. Taylor, G. I., *Proc. Roy. Soc. (London), Ser. A*, **223**, 446 (1954).
7. Tichacek, L. J., C. H. Barkelew, and T. Baron, *AIChE J.*, **3**, 439 (1957).
8. Turner, J. C. R., *British Chem. Engr.*, **9**, 376 (1964).
9. Yablonski, V. S., A. Sh. Asaturyan, and I. Kh. Khizgilov, *Intern. Chem. Engr.*, **2**, 3 (Jan., 1962).
10. Aris, R., et al., *Chem. Eng. Sci.*, **9**, 266 (1959).
11. Bischoff, K. B., et al., *ibid.*, **12**, 69 (1960).
12. Levenspiel, O., and W. K. Smith, *ibid.*, **6**, 227 (1957).
13. Bischoff, K. B., and O. Levenspiel, *ibid.*, **17**, 245 (1962).
14. *Ibid.*, **17**, 257 (1962).
15. Bischoff, K. B., *AIChE J.*, **10**, 584 (1964).
16. Halwagi, M. M., and A. Gomezplata, *ibid.*, 13, 503 (1967).
17. Bischoff, K. B., *Can. J. Chem. Eng.*, **41**, 129 (June, 1963).
18. Cassell, R. E., MS thesis, Univ. Tennessee, Knoxville (1966).
19. Wilks, S. S., "Elementary Statistical Anlysis," pp. 116-117, Princeton Univ. Press, Princeton, N.J. (1948).
20. Koutsky, J. A. and R. J. Adler, *Can J. Chem. Eng.*, **42**, 239 (Dec. 1964).
21. Carter, D. and W. G. Bir, *Chem. Eng. Progr.*, **58**, 40 (March, 1962).

Manuscript received May 29, 1967; revision received January 25, 1968; paper accepted January 26, 1968.

Evaluation of Drying Schedules

RALPH E. PECK and JAE Y. KAUH

Illinois Institute of Technology, Chicago, Illinois

A generalized drying program that can simulate any drying conditions has been solved on a computer. The program includes the variation of humidity, temperature, and wind velocity over drying material. These three variables can be treated as functions of time. The correlations require knowledge of several basic properties of the material to be dried and were solved for the case of one directional heat and mass flow.

The computer calculated results are checked with experimental data. The effective diffusivity and the solid surface resistance to mass transfer were evaluated by data obtained in three experiments.

Solutions for constant drying conditions are presented in graphical form. Variations of such variables as humidity in a drier can be estimated from these curves but the computer program is more reliable.

The process of the drying of solids consists of both the transfer of moisture within the solid and the evaporation of moisture from the surface of the solid into the surrounding medium.

MOISTURE TRANSFER IN THE SOLID PHASE

The transfer of moisture within the drying body is caused by various forces. Such forces may be external pressure, gravity, capillary tension, and molecular diffusion forces. The importance of these various forces is dependent upon the material and drying conditions.

Experimental data for the moisture distribution in various kinds of material have been taken and analyzed by many investigators (*1* to *5*).

In low temperature drying it can be assumed that most of the moisture diffuses through the solid phase as liquid. The simplest form of the drying differential equation in the falling rate period is

$$\frac{\partial \phi}{\partial t} = \alpha \frac{\partial^2 \phi}{\partial x^2} \qquad (1)$$

where α is the effective diffusivity of free moisture within the drying solid, C is the free moisture concentration, weight of free moisture per unit weight of bone dry solid.

Sherwood (*6* to *9*), Newman (*10, 11*), Ceaglske and Hougen (*12*), and others have recommended this equation for predicting the movement of water in a solid or have presented solutions to the equation.

The diffusion equation can be used in all cases where the major resistance is in the gas phase, and in cases where the equation holds in the solid. This equation seems to apply quite well for wood.

MOISTURE TRANSFER ON THE DRYING SURFACE

$\phi = \phi_o$ is taken as an initial condition. The boundary conditions at the surface $x = L$ are taken as

$$-\alpha \rho_o \frac{\partial \phi}{\partial x} = k_g \gamma (P_s - P_g) \qquad (2)$$

and

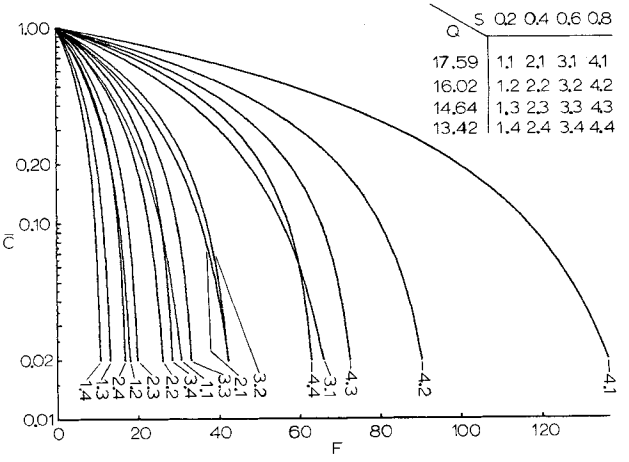

Fig. 1. Dimensionless drying curves at $Z = 1.0$.

Jae Y. Kauh is with Union Carbide Co., South Charleston, West Virginia.